Redox Biology 48 (2021) 102192

Contents lists available at ScienceDirect

Redox Biology

journal homepage: www.elsevier.com/locate/redox

Compensatory role of endogenous sulfur dioxide in nitric oxide deficiency-induced hypertension

Yunjia Song [a,1], Jiaru Song [a,1], Zhigang Zhu [a], Hanlin Peng [a], Xiang Ding [b], Fuquan Yang [b], Kun Li [c], Xiaoqi Yu [c], Guosheng Yang [d], Yinghong Tao [d], Dingfang Bu [e], Chaoshu Tang [f], Yaqian Huang [a], Junbao Du [a,f], Hongfang Jin [a,*]

[a] Department of Pediatrics, Peking University First Hospital, Beijing, China
[b] Key Laboratory of Protein and Peptide Pharmaceuticals & Laboratory of Proteomics, Institute of Biophysics, Chinese Academy of Sciences, Beijing, 100101, China
[c] Key Laboratory of Green Chemistry and Technology, Ministry of Education, College of Chemistry, Sichuan University, Chengdu, 610064, China
[d] Laboratory Animal Facility, Peking University First Hospital, Beijing, 100034, China
[e] Central Laboratory, Peking University First Hospital, Beijing, 100034, China
[f] Key Laboratory of Molecular Cardiology, Ministry of Education, Beijing, China

ARTICLE INFO

Keywords:
Sulfur dioxide
Aspartate aminotransferase
S-Nitrosylation
Endothelial cells
Remodeling

ABSTRACT

Objective: This study aimed to determine the communicational pattern of gaseous signaling molecules sulfur dioxide (SO_2) and nitric oxide (NO) between vascular endothelial cells (VECs) and vascular smooth muscle cells (VSMCs), and elucidate the compensatory role and significance of endogenous SO_2 in the development of hypertension due to NO deficiency.

Approach and results: Blood pressure was monitored by the tail-cuff and implantable physiological signal telemetry in L-nitro-arginine methyl ester (L-NAME)-induced hypertensive mice, and structural alterations of mouse aortic vessels were detected by the elastic fiber staining method. L-NAME-treated mice showed decreased plasma NO levels, increased SO_2 levels, vascular remodeling, and increased blood pressure, and application of L-aspartate-β-hydroxamate, which inhibits SO_2 production, further aggravated vascular structural remodeling and increased blood pressure. Moreover, in a co-culture system of HAECs and HASMCs, NO from HAECs did not influence aspartate aminotransferase (AAT)1 protein expression but decreased AAT1 activity in HASMCs, thereby resulting in the inhibition of endogenous SO_2 production. Furthermore, NO promoted S-nitrosylation of AAT1 protein in HASMCs and purified AAT1 protein. Liquid chromatography with tandem mass spectrometry showed that the Cys192 site of AAT1 purified protein was modified by S-nitrosylation. In contrast, dithiothreitol or C192S mutations in HASMCs blocked NO-induced AAT1 S-nitrosylation and restored AAT1 enzyme activity.

Conclusion: Endothelium-derived NO inhibits AAT activity by nitrosylating AAT1 at the Cys192 site and reduces SO_2 production in HASMCs. Our findings suggest that SO_2 acts as a compensatory defense system to antagonize vascular structural remodeling and hypertension when the endogenous NO pathway is disturbed.

1. Introduction

Hypertension, characterized by increased blood pressure in the arteries of the body circulation and sustained increase in vascular tone, is a latent risk factor for several cardiovascular diseases and chronic renal failure. By 2025, 1.56 billion people worldwide are expected to be affected by hypertension [1,2]. Despite numerous experimental studies, the exact pathogenesis of hypertension is still in its infancy. Therefore, exploring the pathogenesis of hypertension is an important scientific topic in life science and medicine presently.

Nitric oxide (NO) is an indispensable gas signaling molecule in the body, produced by L-arginine catalyzed by nitric oxide synthase (NOS). Endothelial-derived NO is a potent vasodilator substance and has a significant impact on the maintenance of homeostasis in the cardiovascular system of the body by activating soluble guanylate cyclase and producing intracellular cyclic guanosine phosphate, which leads to smooth muscle relaxation [3–5]. Several animal studies demonstrate

* Corresponding author. Department of Pediatrics, Peking University First Hospital, No. 1, Xi'an-men Street, West District, Beijing, 100034, China.
E-mail address: jinhongfang51@126.com (H. Jin).
[1] These authors contributed equally to this work.

https://doi.org/10.1016/j.redox.2021.102192
Received 15 July 2021; Received in revised form 11 November 2021; Accepted 17 November 2021
Available online 18 November 2021

Abbreviations

AAT	aspartate aminotransferase
DTT	dithiothreitol
eNOS	endothelial nitric oxide synthase
HAECs	human aortic endothelial cells
HASMCs	human aortic smooth muscle cells
HDX	L-aspartate-β- hydroxamate
L-NAME	L-nitro-arginine methyl ester
NO	nitric oxide
NOS	nitric oxide synthase
SBP	systolic blood pressure
SHR	spontaneously hypertensive rats
SNP	sodium nitroprusside
SO_2	sulfur dioxide

that restraint of constitutively expressed endothelial nitric oxide synthase (eNOS), which interrupts NO production, leads to an increase in blood pressure and the development of hypertension [6,7]. Clinical data suggest that systemic NO production is reduced in hypertensive patients compared to normotensive controls. When NO biosynthesis is reduced or inactivated, NO bioavailability is reduced; reduced NO bioavailability leads to a decreased diastolic function of the vascular wall and is a pivotal factor for the development of hypertension [8]. In addition, endogenous sulfur dioxide (SO_2), a novel endogenous gasotransmitter, is produced with L-cysteine as a substrate and is catalyzed by aspartate aminotransferase (AAT). The endogenous SO_2/AAT pathway is present in alveolar epithelial cells, vascular endothelial cells, vascular smooth muscle cells, fibroblasts, cardiomyocytes, and adipocytes and is a contributory factor in the regulation of cardiovascular homeostasis [9–14]. Our group has proposed for the first time that endogenous SO_2 acts as a fourth gaseous signaling molecule in cardiovascular regulation and is involved in maintaining normal cardiovascular structure [15–18]. Other studies also showed that plasma SO_2 level in serum was significantly decreased in spontaneously hypertensive rats (SHR), while, supplementation of SO_2 donor significantly inhibited hypertension in SHRs [19]. SO_2 donor promoted the relaxation of isolated rat aortic rings in a concentration-dependent manner, while L-aspartate-β-hydroxamate (HDX), an inhibitor of AAT, inhibited endogenous SO_2 production and subsequently caused vasoconstriction [20]. The abovementioned findings suggest that SO_2, as a bioactive molecule, exerts a powerful effect on the regulation of vasodilatory function.

Accumulating evidence indicates that the interactions amongst members of different bioactive substance families, such as peptides, amino acids, and gaseous signaling molecules, play a critical regulatory role in vascular regulation [21–23]. However, the integrated regulatory role of gaseous signaling molecules in the development of hypertension and its mechanisms remain unclear. Similar to SO_2, NO, a gaseous signaling molecule, has various biological effects, such as vasodilation, antioxidant, and anti-inflammatory activities [14,15,24]. Interestingly, Li et al. found that low concentrations (3 or 5 nM) of sodium nitroprusside (SNP) increased the vasodilatory effect of SO_2 by approximately 6-fold [25], and Lu et al. found that SO_2 increased the NO level of SHR aorta and enhanced the vasodilatory response of SHR aorta to SNP [26], suggesting that NO and SO_2 possibly have a synergistic vasodilatory effect. While, the effect of endogenous NO on endogenous SO_2 production and its role in the pathogenesis of hypertension remains unclear. Gaseous signal molecules can freely pass through the cell membrane and exert a regulatory effect in adjacent cells through a paracrine mode. Therefore, we hypothesized that the interaction between NO and SO_2 might mediate intercellular communication between human aortic endothelial cells (HAECs) and human aortic smooth muscle cells (HASMCs).

Therefore, this study was undertaken to explore the effect of endothelial-derived NO on endogenous SO_2 production in HASMCs and its mechanisms to elucidate the significance of NO–SO_2-based intercellular communication between HAEC and HASMCs in the development of hypertension and vascular remodeling.

2. Materials and methods

2.1. Animal model and capsule osmotic pressure pump implantation

Mice were purchased from Beijing Viton Lever Experimental Animal Center and housed in the Experimental Animal Center of Peking University First Hospital. During the experiments, mice were fed and watered freely, and the 12 h/12 h circadian rhythm was maintained. During the experimental operation, the animal management rules of the Ministry of Health of the People's Republic of China were strictly observed and approved by the Animal Research Ethics Committee of Peking University First Hospital (Ethics No.: 201747). Thirty-two male C57BL/6J mice weighing 20–25 g were randomly distributed into the following 4 groups (8 mice in each group): The control group comprised mice with an intraperitoneal injection of saline; the L-nitro-arginine methyl ester (L-NAME) group included mice with a subcutaneous dorsal surgery with a capsule osmolarity pump preloaded with L-NAME (100 mg/kg); the L-NAME + HDX group consisted of mice with a subcutaneous dorsal surgery with a capsule osmolarity pump preloaded with L-NAME (100 mg/kg) and daily intraperitoneal injection of HDX (25 mg/kg); the HDX group included mice with a daily intraperitoneal injection of HDX (25 mg/kg) for 8 weeks.

These mice were monitored weekly for blood pressure changes. The capsule osmotic pressure pump was implanted with L-NAME (100 mg/kg) solution preloaded in the capsule osmotic pressure according to the instructions, and the pump was administered subcutaneously on the back of the mice after blood pressure measurement. Mice were anesthetized through intraperitoneal injection of 0.5% sodium pentobarbital (100 μl/10 g) and fixed in a prone position. The skin and subcutaneous tissue were cut in the middle of the scapula posteriorly, and the capsule osmotic pressure pump was then carefully placed subcutaneously on the back. The subcutaneous tissue and skin were sutured together, and 200 μl of saline was injected intraperitoneally. The mice were placed on an electric blanket (37°C) for observation after surgery and were then placed back in the cage after the mice could move freely.

2.2. Tail-cuff method for blood pressure measurement in mice

The mice were placed in a quiet environment, fixed in a mouse bag, and put into a heat preservation tube to keep warm. The cuff was put on the root near the tail of the mouse, and the mouse was adapted for a while. After the blood pressure of mice was stable, the tail-cuff was pressed automatically to measure the blood pressure 3 times, and the mean value was calculated.

2.3. Implantable telemetry for blood pressure detection in mice

Mice were anesthetized through intraperitoneal injection of 0.5% sodium pentobarbital (100 μl/10 g). Then, the mice were fixed on the operating table in a supine position with an elastic band. Along the median neck incision, the left common carotid artery was carefully separated under a body vision microscope, and the catheter of the implant sub (soaked in saline for 15–30 min before surgery) was gently fed into the vessel for 1–2 cm, and the implant sub was fixed to the abdominal muscle of the mice. After one week of postoperative observation, when the mice were in normal mental state and activity, the implantable radio telemetry devices were opened and programmed to monitor the blood pressure of the mice every 1 min for 48 h. The blood pressure monitoring data were saved.

2.4. Mouse aortic elastic fiber staining

The sections were sequentially placed in three separate xylene tanks, each tank for 10 min, and then dewaxed in anhydrous ethanol, 95% ethanol, and 75% ethanol for 10 min. Next, the sections were immersed in a staining tank with Weigert resorcinol magenta staining solution for 3 h at 25°C and then washed in deionized water three times (10 min each). The background staining of the cell pulp was removed with 95% ethanol, and the sections were transferred to anhydrous ethanol for 10 min, followed by incubation with xylene three times for 10 min. The slices were sealed up with resin, left at room temperature for 2–3 days, and observed under a microscope. The morphometric indices including aortic median area and thickness were detected with the Optilab algorithm on LeicaQ550cw cytogenic workstation. The median area was defined as the area surrounded by the internal and external elastic lamina of the aorta. For the measurement of the aortic median thickness, each aorta section was gauged at four points 0, 3, 6, and 9 o'clock clockwise and then the average value was calculated.

2.5. Mouse arterioles in brown fat elastic fiber staining

The brown fat tissue on the back of mice was fixed with 4% polymethyl and embedded in paraffin. The sections were soaked in xylene to dewax, and then rehydrated in gradient ethanol as the abovementioned protocol. Next, the sections were stained with the Verhoeff staining solution, a mixture of alcohol hematoxylin, ferric chloride, and iodine solution for 30 min. The differentiation solution slightly differentiated the background. The sections were stained with Van Gieson solution (saturated picric acid: the acidic magenta in a volume ratio of 9:1) for 1–3 min and washed quickly with water. Finally, the sections were sequentially soaked with anhydrous ethanol and xylene for 1–5 min, and sealed with neutral resin. The elastic fibers are purple-black and the collagen fibers are red. Images were acquired and analyzed using Leica Q550 CW. Each section was selected for 3 different fields of view under a microscope.

2.6. Immunofluorescence assay of collagen I and III

Collagen III protein expression in primary HASMCs was detected by immunofluorescence assay. HASMCs were washed with PBS twice (5 min each time). Cells were fixed with 4% paraformaldehyde for 20 min. After washing with PBS, cells were incubated with 200 μl of punching solution (10 mL of PBS, 0.5 g of bovine serum albumin, and 30 μl of Triton X-100) at 37°C for 0.5–1 h. They were then incubated with primary antibody (dilution: 1:50; 50 μl/well) in punching solution at 37°C for 1 h and then at 4°C for 8 h. Cells were subsequently incubated with secondary antibodies for 2 h at 37°C (red fluorescent mouse secondary antibody; diluted 1:300 with PBS). The red fluorescent signal represents the collagen I or III protein in the cells when observed using laser confocal microscopy.

2.7. Colorimetric detection of NO

NO levels in cell supernatant and mouse plasma were detected with a nitric oxide assay kit (Beyotime Biotechnology). HAECs supernatant (50 μl) or mouse plasma (50 μl) was added to a 96-well plate. Griess Reagent I and II (50 μl) were added sequentially, and absorbance was measured at 540 nm. The concentrations of NO in these samples were computed according to the standard curve.

2.8. Western blotting of AAT1, eNOS, collagen I and III

Cells or tissues were lysed in RIPA buffer (Beyotime, China). Equal quantities of proteins were separated using 10% SDS-PAGE gel and transferred to nitrocellulose membranes, and the membranes were then blocked with a closure solution containing 5% milk. The primary antibodies and their dilutions used were as follows: anti-AAT1 (1:1000; Sigma, USA), anti-collagen I (1:1000; Abcam, USA), anti-collagen III (1:500; Abcam, USA), anti-eNOS (1: 500; Santa Cruz, USA), and anti-GAPDH (1:5000; Kangcheng, China). Bands were photographed using chemiluminescence reagents with a FluorChem M MultiFluor system (Protein Simple, USA), and the optical density of the bands was quantified using the multi-band analysis function of AlphaEaseFC (Alpha, USA) software.

2.9. Determination of AAT activity by colorimetric assay

AAT activity of aorta tissue, cells, and purified proteins of porcine AAT1 was measured as described previously [27] according to the instructions of the AAT activity assay kit (Nanjing Jiancheng, Nanjing, China). The AAT activity of aorta tissue and cells was corrected for homogenate protein concentration and was expressed as U/g. Purified protein AAT activity was measured and expressed as Carmen's units/g.

2.10. Detection of SO_2 by high-performance liquid chromatography (HPLC)

Sodium borohydride (dissolved with 50 mM Tris-HCl [pH 8.5]; 212 μM) was added to the samples or sulfite standards (0, 1, 2, 5, 10, and 20 μM) and incubated for 0.5 h at 25°C. Then, 70 mM monobromobimane was added, and the mixture was incubated at 42°C for 10 min. The supernatant fluid was mixed with 2.0 M Tris-HCl and centrifuged at room temperature at 12,000 g for 10 min. The mouse plasm and supernatant fluid were transferred to a special brown glass vial and analyzed by HPLC (Agilent 1100 series, USA). The standard curve was prepared according to the sulfite standard and the corresponding peak area, and the SO_2 level of each specimen was calculated by substituting the peak area based on the standard curve.

2.11. Cell culture

HASMCs (Lifeline, USA) were grown in the vascuLife® SMC complete medium (Lifeline, USA) containing 5% fetal bovine serum, 30 mg/mL gentamicin, 15 μg/mL amphotericin B, 5 ng/mL rh basic FGF, 5 μg/mL rh insulin, 10 mM L-glutamine, 50 μg/mL ascorbic acid, and 5 ng/mL rh EGF. HAECs (Lifeline, USA) were grown in the vascuLife® VEGF endothelial complete medium (Lifeline, USA) containing 2% fetal bovine serum, 30 mg/mL gentamicin, 15 μg/mL amphotericin B, 5 ng/mL rh VEGF, 5 ng/mL rh basic FGF, 1 μg/mL hydrocortisone hemisuccinate, 50 μg/mL ascorbic acid, 10 mM L-glutamine, 15 ng/mL rh IGF-1, 5 ng/mL rh EGF, and 0.75 U/mL heparin sulfate. Cells were cultured with 5% CO_2 at 37°C and starved for 6 h before drug treatment. HASMCs were treated with NO donor SNP for 2 h and divided into control, 50 μM, 100 μM, and 200 μM groups.

2.12. Preparation of eNOS-deficient HAECs

HAECs were cultured and infected with lentivirus carrying shRNA targeting eNOS gene (1×10^5 TU/ml) and polybrene (5 μL/ml) at 70% confluence. After 24-h infection, cells were cultured in a fresh medium for 72 h. HAECs were treated with 4 μg/mL puromycin for 2 weeks to screen stable HAECs infected with eNOS shRNA lentivirus.

2.13. Plasmid transfection in HASMCs

AAT1-C192S (cysteine [site 192] mutates to serine) plasmid or AAT1-WT(wild-type) plasmid were transfected into HASMCs using JetPEI reagent (Polyplus-transfection, France) following manufacturer's instructions for 12 h before treatment.

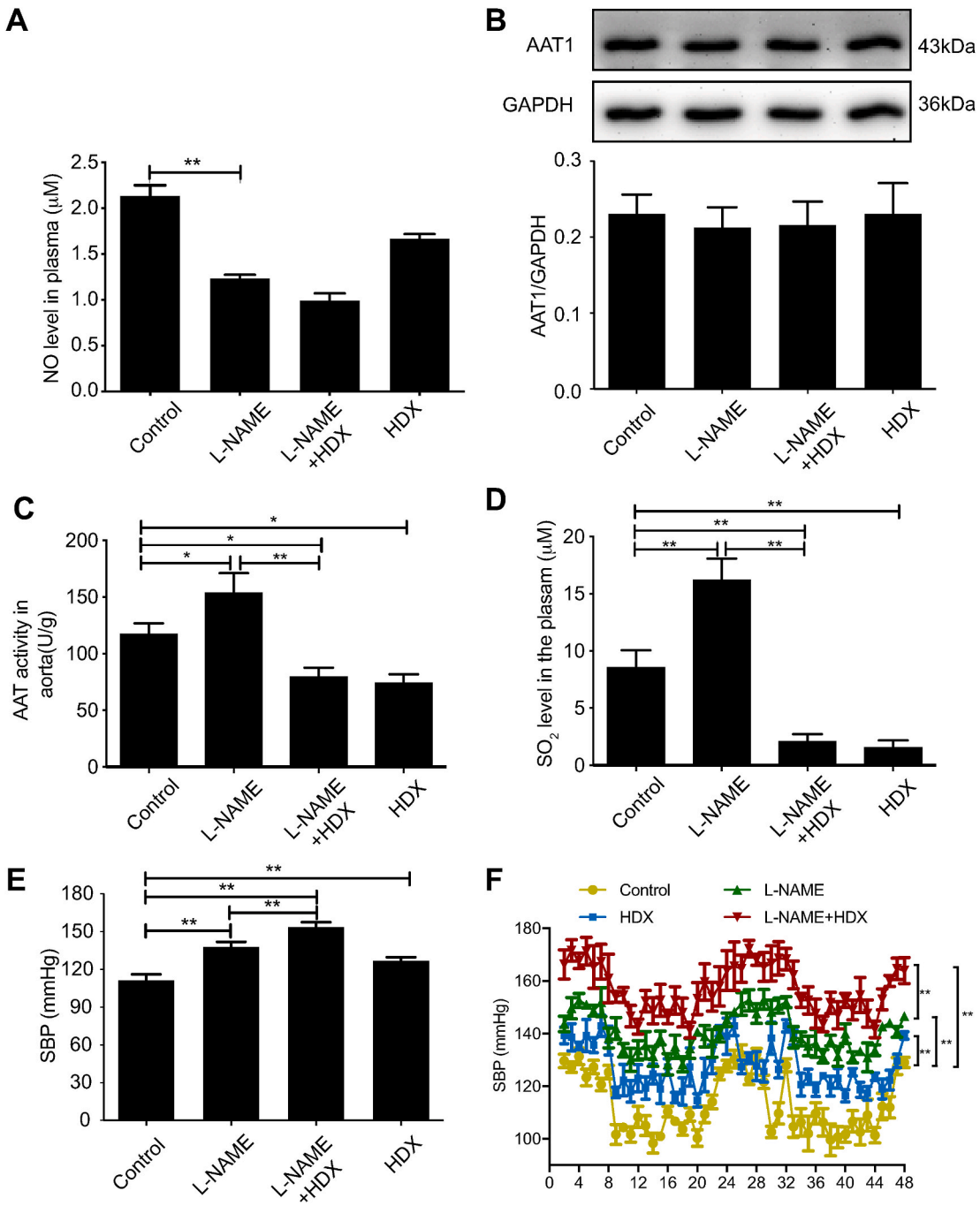

Fig. 1. Endogenous SO_2 pathway compensates disturbed endogenous NO generation to protect against hypertension. **A**, Colorimetric assay of plasma NO content in mice (n = 8). **B**, Western blotting analysis to detect the expression of AAT1 protein in mouse aortic tissues (n = 8). **C**, Colorimetric assay of AAT activity in mouse aortic tissues (n = 8). **D**, Colorimetric assay to determine SO_2 in mouse plasma (n = 8). **E**, Blood pressure measurement in mice by the tail-cuff method (n = 8). **F**, Blood pressure monitoring in mice by implantable telemetry (n = 3). Data are expressed as mean ± SEM. $^*P < 0.05$, $^{**}P < 0.01$. AAT, aspartate aminotransferase; NO, nitric oxide; SO_2, sulfur dioxide.

2.14. Primary HAECs and HASMCs co-culture

HAECs stably transfected with eNOS shRNA lentivirus were inoculated in the lower chamber of a transwell 6-well plate, and 1.5 mL of vascular endothelial cell complete medium was added. Meanwhile, HASMCs were inoculated in the upper chamber of the transwell 6-well plate. Then, 1.5 mL of vascular smooth muscle cell complete medium was added, and cells were incubated in an incubator containing 5% CO_2 at 37 °C. Primary HAEC and HASMC co-cultures were used and divided into the empty virus transfection group, eNOS shRNA lentiviral infection group, and eNOS shRNA lentiviral infection + HASMCs HDX group, in which 100 μM HDX was added for 24 h.

2.15. In situ detection of endogenous SO_2 levels in cells by fluorescent probes

SS-1 is a chemoselective fluorescent probe for *in situ* detection of SO_2, developed and generously given by Prof. Xiaoqi Yu and Prof. Kun Li from Sichuan University [28]. The threshold of detecting SO_2 derivatives in PBS buffer by the SS-1 probe reached 92 nM.

Simultaneously, the SS-1 probe was reported to selectively react with SO_2 and exhibit low cytotoxicity [28]. Cells were cultured in chambers, incubated with the fluorescent probe of SO_2 for 0.5 h, rinsed with PBS 3 times, and then fixed with 4% paraformaldehyde for at least 10 min. Cells were rinsed as described above and added an appropriate concentration of DAPI to visualize nuclear DNA. Immunofluorescence results were obtained using a confocal microscope (TCS SP5, Leica Microsystems, Germany), with blue fluorescence representing the nucleus and green fluorescence representing the SO_2 level. The signal intensity of fluorescence was measured using Image J (NIH, USA) software.

2.16. Analysis of enzymatic kinetic properties of AAT1

Porcine AAT1 purified protein (Sigma, USA) (75 ng) was treated with 0.1 mM SNP or ddH_2O for 0.5 h at 37°C and then assorted with various concentrations of matrix solution (L-aspartic acid and α-ketoglutaric acid in a fresh configuration at a 1:100 M ratio, with α-ketoglutaric acid concentrations of 100, 50, 25, 12.5, 6.25, and 2.5 μM, respectively). The mixed liquor was incubated at 37 °C for 30 min. AAT activity was detected by the AAT activity assay kit. The Vmax and Km values of AAT1 protein were calculated from the Eadie-Hofstee plot, a transformed form of the Michaelis-Menten equation [29].

2.17. Biotin switch assay for S-nitrosylation modifications detection

Cells were rinsed with pre-cooled PBS three times, and Hens 1 solution (0.25 M Hepes, 100 μM neocuproine, 1‰ SDS, 1% Triton X-100, protease inhibitors, phosphatase inhibitors, 1 mM EDTA, and PMSF) was then added. Cells were incubated on ice for 0.5 h, and 10 μl of the supernate was retained as basic protein. The remaining supernate was incubated with a final concentration of 0.02 M MMTS for 20 min at 50 °C, and proteins were resuspended by precipitation with acetone followed by the addition of Hens 1 solution and a final concentration of 5 mM ascorbic acid and 1 mM Biotin-HPDP. Subsequently, 50 μl of NeutrAvidinTM was added into the mixture and incubated at 4°C for 8 h. The beads were rinsed 3 times with Hens solution, 1 mM EDTA, and 0.5% Triton X-100. Proteins were subjected to western blotting to detect protein S-nitrosylation modifications.

2.18. In situ detection of AAT1 S-nitrosylation levels by fluorescent probe assay

AAT1 S-nitrosylation level was measured by fluorescent probe assay according to instructions of the cellular protein S-nitrosylation modification detection kit (Cayman, USA). Confocal microscopy was applied to observe and take pictures. Blue light shows the nucleus, green fluorescence indicates nitrosylated protein, red fluorescence shows AAT1 protein, and co-localization of two fluorescence fusions represents the nitrosylated modified AAT1 protein.

2.19. Detection of AAT1 S-nitrosylation by liquid chromatography-mass spectrometry (LC-MS/MS)

Purified AAT1 protein was prepared in 100 μl of PBS, and 100 μM NO was then added; the mixture was incubated in a water bath for 0.5 h at 37°C with gentle shaking. A final concentration of 20 mM MMTS was added into the mixed liquids and incubated at 50°C with shaking for 20 min. After protein precipitation with acetone, the protein samples were resuspended by adding Hens 1 solution and a final concentration of 5 mM ascorbic acid and 1 mM Biotin-HPDP, and the solution was incubated for 1.5 h. After the addition of a non-reducing loading buffer, the protein samples were separated with 10% SDS-PAGE gel. The protein gel bands were stained with Coomassie Brilliant Blue R-250, followed by in-gel digestion, and the acetonitrile-extracted peptide mixture was analyzed by liquid chromatography-linear ion trap-orbitrap mass

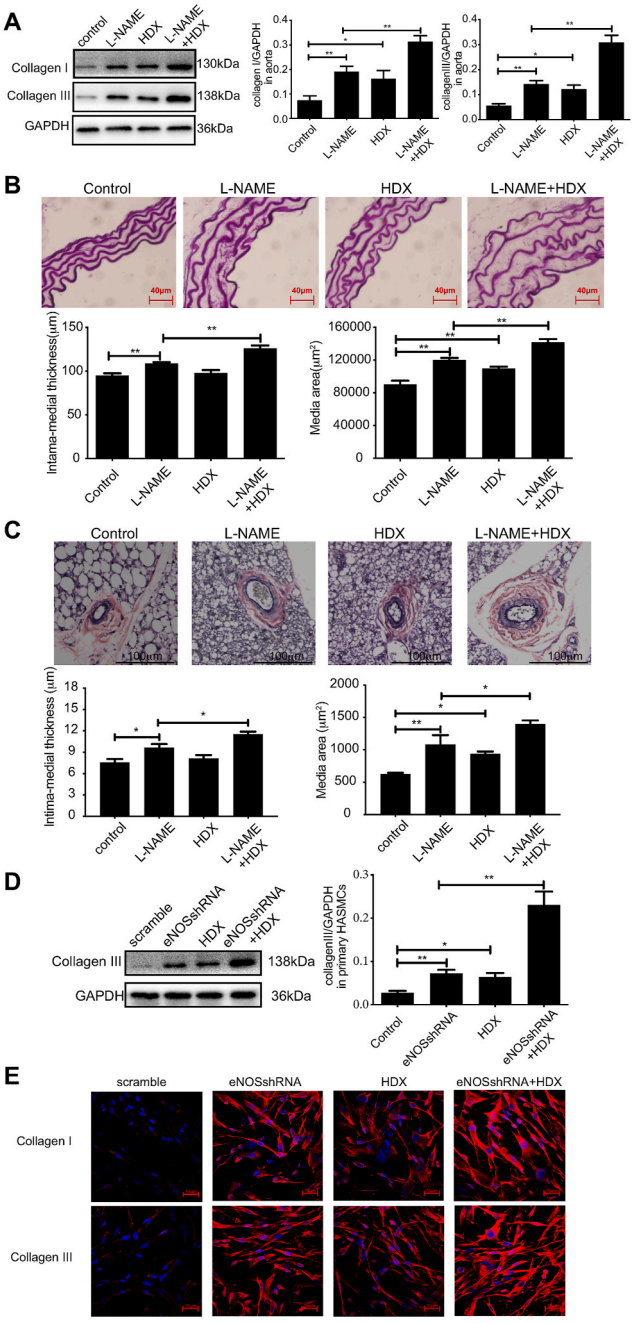

Fig. 2. Endogenous SO_2 pathway compensates disturbed endogenous NO generation to protect against vascular structural remodeling **A**, Western blot analysis to detect collagen I and III protein expression in mouse aortic tissues (n = 8). **B**, Elastic fiber staining method to detect the median area and thickness in the mouse aortic section (n = 8). Scale bar, 40 μm. **C**, Verhoeff's-Van-Gieson staining of arterioles in mouse brown fat tissues (n = 8). Scale bar, 100 μm. **D**, Primary HAECs were transfected with scramble or eNOS shRNA lentivirus and co-cultured with primary HASMCs. Primary HASMCs were incubated with 100 μM HDX in the culture supernatant for 24 h. Western blotting analysis was performed to detect the protein expression of collagen III in primary HASMCs in the co-culture experiment (n = 10). **E**, Primary HAECs were transfected with scramble or eNOS shRNA lentivirus and co-cultured with primary HASMCs. Primary HASMCs were incubated with 100 μM HDX in the culture supernatant for 24 h. Collagen I and III protein expression in primary HASMCs was detected by immunofluorescence in the co-culture experiment (n = 9). The nucleus and collagen I/III are indicated by blue and red fluorescence, respectively. Scale bar, 30 μm $^{**}P < 0.01$. HDX, L-aspartate-β-hydroxamate; NO, nitric oxide; SO_2, sulfur dioxide. (For interpretation of the references to color in this figure legend, the reader is referred to the Web version of this article.)

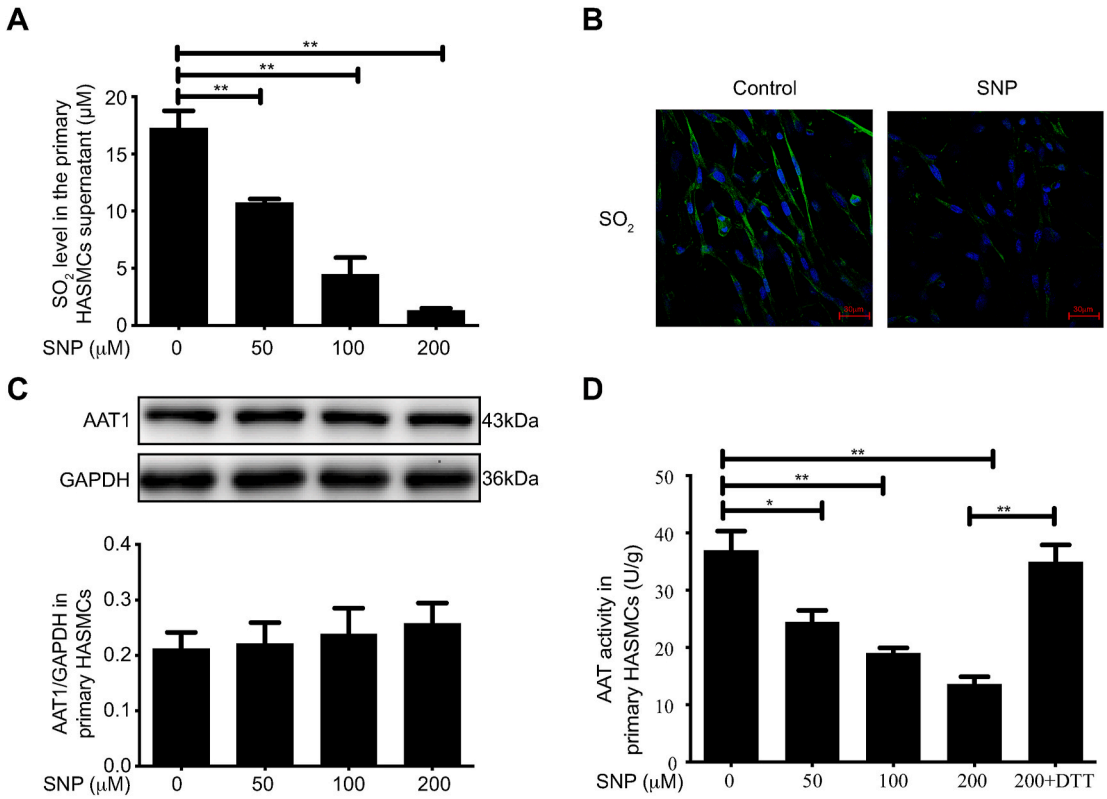

Fig. 3. NO donor inhibits endogenous SO_2 production by suppressing AAT1 activity in primary HASMCs. **A**, Primary HASMCs were treated by varying concentrations of SNP (0, 50, 100, or 200 μM) for 2 h. SO_2 content in the supernatant in primary HASMCs was detected by HPLC. **B**, Primary HASMCs were treated with 100 μM SNP for 2 h, and endogenous SO_2 content in primary HASMCs was detected by the SO_2 fluorescence probe method. The nucleus is indicated by blue fluorescence, and SO_2 by green fluorescence. Scale bar, 30 μm. **C**, Primary HASMCs were treated with various concentrations of SNP (0, 50, 100, or 200 μM) for 2 h, and AAT1 protein expression was detected in primary HASMCs by western blotting analysis. **D**, Primary HASMCs were treated with various concentrations of SNP (0, 50, 100, or 200 μM) for 2 h or with 200 μM SNP for 1 h and then DTT (100 μM) for 1 h. Colorimetric assay was used to detect AAT activity in primary HASMCs. $^*P < 0.05$, $^{**}P < 0.01$. n = 9–12. Data are expressed as mean ± SEM. NO, nitric oxide; SNP, sodium nitroprusside; SO_2, sulfur dioxide. (For interpretation of the references to color in this figure legend, the reader is referred to the Web version of this article.)

spectrometer. Data analysis was performed using Proteome Discoverer (version 1.4.0.288, Thermo Fischer Scientific) software.

2.20. Statistical analysis

All data are presented as mean ± SEM. Both IBM SPSS 22.0 and Graphpad Prism 8.0 were used for statistical analysis. The two-tailed Student's *t*-test was adopted to compare two groups. One-way ANOVA followed by LSD postdoc analysis was used to compare the data among multiple groups. Statistical significance was regarded as $P < 0.05$.

3. Result

3.1. Endogenous SO_2 compensates disturbed endogenous NO generation to protect against hypertension

We treated mice with L-NAME, a NOS inhibitor, to construct a hypertensive mouse model [30]. Compared with the control group, plasma NO level was decreased by 42.11% ($P < 0.01$) without any change in aortic AAT1 protein expression, while the aortic AAT activity was increased by 31.35% ($P < 0.05$) with the subsequently increased SO_2 level by 89.46% ($P < 0.01$) in the L-NAME group (Fig. 1A–D). At the same time, systolic blood pressure (SBP) measured by tail-cuff method was significantly increased by 20.53% ($P < 0.01$) in the L-NAME group compared with the control group (Fig. 1E). Furthermore, HDX, an AAT inhibitor, was used to inhibit the generation of endogenous SO_2 and explore the significance of L-NAME-upregulated SO_2/AAT pathway. The results showed that the aortic AAT activity and SO_2 level were decreased by 36.55% ($P < 0.05$) and 82.10% ($P < 0.01$), respectively, but the SBP was elevated by 14% in the mice of the HDX group compared with the control group (Fig. 1C–E). When HDX was co-administered in L-NAME-treated mice, plasma NO content did not change significantly; however, aortic tissue AAT activity was decreased by 48.29% ($P < 0.01$) with the subsequent decrease in SO_2 content by 87.11% ($P < 0.01$), and the SBP was further increased by 13.33% ($P < 0.01$) (Fig. 1A–E). The results of SBP real-time monitoring values by implantable telemetry in awake unrestrained mice were similar to those of the tail-cuff method (Fig. 1F). The above findings suggest that the endogenous SO_2 pathway might act as a compensatory defense system to antagonize hypertension in response to disturbed endogenous NO generation.

3.2. Endogenous SO_2 compensates disturbed endogenous NO generation to protect against vascular structural remodeling

In the aorta tissue of mice, collagen I and collagen III protein expressions were increased by 154.87% and 158.18%, respectively, and the median thickness and area were increased by 14.69% and 33.05%, respectively, in L-NAME-treated mice compared with control mice (P all<0.01). HDX treatment further upregulated the protein expression of collagen I and collagen III, the media thickness and area by 64.05%, 116.90%, 15.92%, and 17.08% in the L-NAME + HDX group, respectively (P all <0.01). While compared with the control group, the expression of collagen I, collagen III and the media area in the mice of the HDX group were elevated by 116.06% ($P < 0.05$), 120.22% ($P < 0.05$), and 21.73% ($P < 0.01$), respectively (Fig. 2A and B). In the arterioles in brown fat of mice, L-NAME treatment increased the media

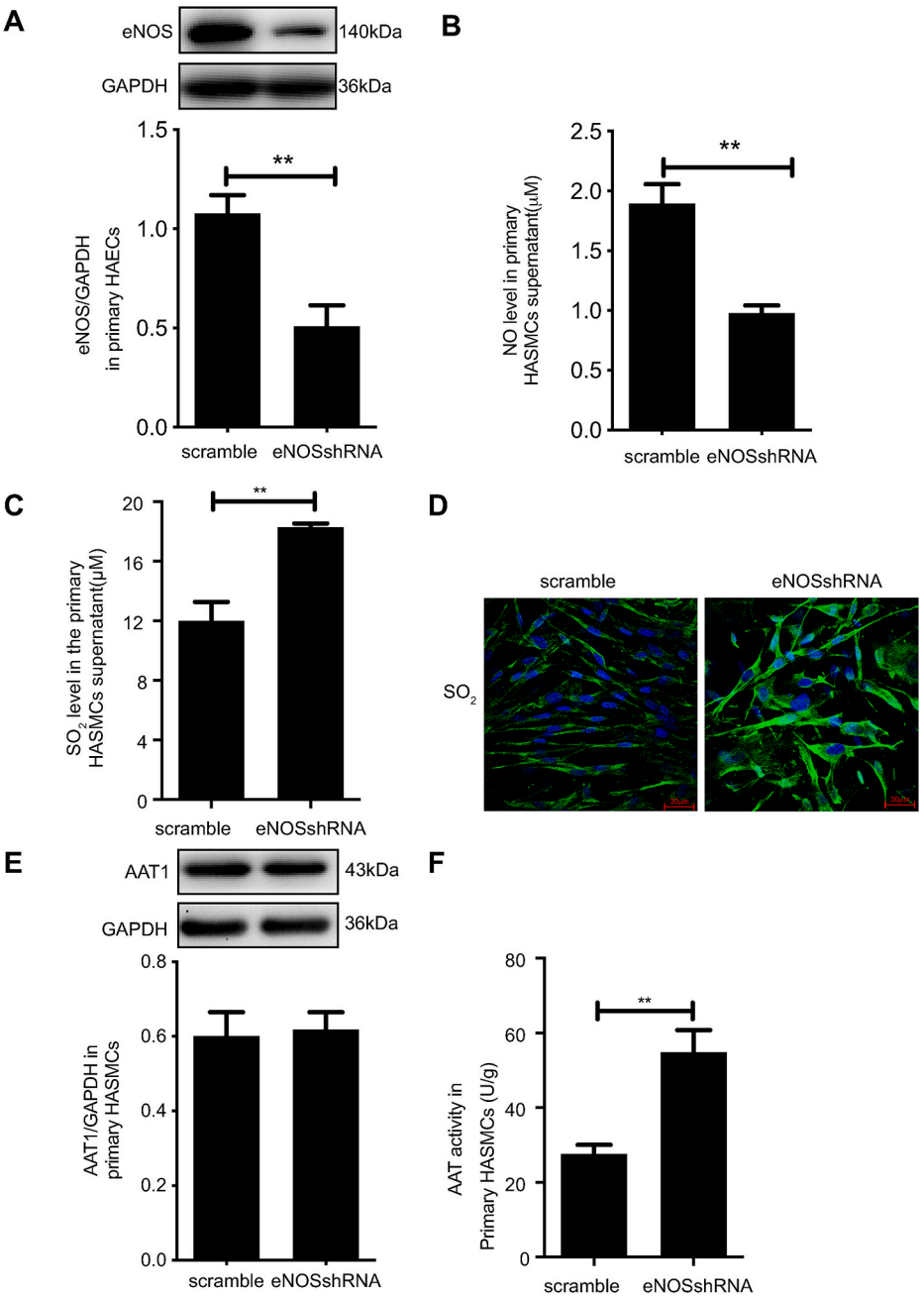

Fig. 4. eNOS knockdown facilitates endogenous SO_2 production by promoting AAT1 activity in primary HASMCs. Primary HAECs were transfected with scramble or eNOS shRNA lentivirus, and the stably transfected lentiviral HAECs were co-cultured with HASMCs. **A**, Western blotting analysis to detect eNOS protein expression in primary HAECs in the co-culture system. **B**, A colorimetric assay to detect the supernatant NO content in the primary HAECs in the co-culture system. **C**, HPLC method for determining SO_2 in the supernatant in primary HASMCs in the co-culture system. **D**, SO_2 fluorescence probe to detect endogenous SO_2 in primary HASMCs in the co-culture system. The nucleus is indicated by blue fluorescence, and SO_2 by green fluorescence. Scale bar, 20 μm. **E**, Western blotting analysis to detect AAT1 protein expression in primary HASMCs in the co-culture system. **F**, Colorimetric assay to detect AAT activity in primary HASMCs in the co-culture system. $^{**}P < 0.01$. n = 9–12. Data are expressed as mean ± SEM. HDX, L-aspartate-β-hydroxamate; NO, nitric oxide; SO_2, sulfur dioxide. (For interpretation of the references to color in this figure legend, the reader is referred to the Web version of this article.)

thickness and area of arterioles in the control mice by 27.65% ($P < 0.05$) and 72.62% ($P < 0.01$), respectively. The intervention of HDX performed on the L-NAME-treated mice further upregulated the media thickness and area of arterioles by 19.65% and 29.34%, respectively (P all <0.05). While, the media area of arterioles in the mice of HDX group was elevated by 49.73% compared with the control group ($P < 0.05$) (Fig. 2C). The above findings suggested that the change of vascular remodeling in the resistance arteries was in accordance with that in the aortas.

The results of co-culture of primary HAECs and primary HASMCs showed that compared with the scramble group, collagen III protein expression was increased by 167.41% ($P < 0.01$), collagen I and III protein fluorescence signals were enhanced in primary HASMCs co-cultured with eNOS knock-downed primary HAECs. Furthermore, compared with the eNOS shRNA group, the expression of collagen III protein was further increased by 218.56% ($P < 0.01$), collagen I and III protein fluorescence signals were further enhanced after HDX intervention in primary HASMCs. Compared with the scramble group, collagen III protein expression was increased by 135.73% ($P < 0.05$), collagen I and III protein fluorescence signals were enhanced in HDX-treated primary HASMCs (Fig. 2D and E). The results suggest that the endogenous SO_2 pathway might act as a compensatory defense system against vascular structural remodeling in response to disturbed endogenous NO generation.

3.3. *NO donor inhibits endogenous SO_2 production by suppressing AAT1 activity in primary HASMCs*

To investigate the influence of NO on endogenous SO_2 production in primary HASMCs, primary HASMCs were treated with different concentrations (0, 50, 100, and 200 μM) of the NO donor SNP. HPLC results showed that SO_2 levels in the supernatants of primary HASMCs treated

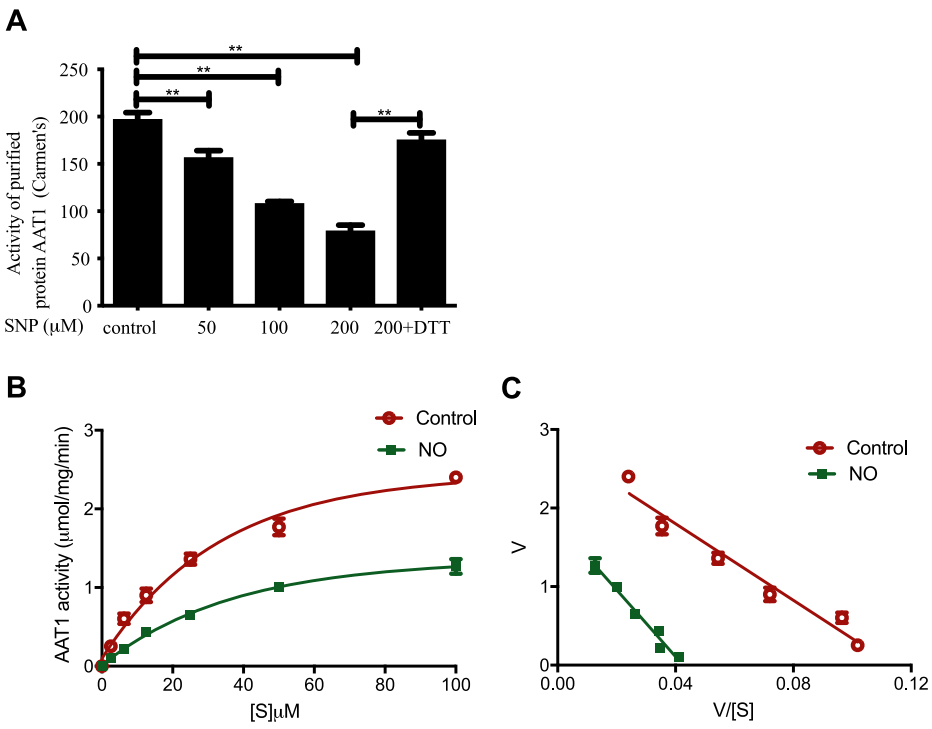

Fig. 5. NO directly inhibits the activity of AAT1 purified protein and affects kinetic characteristics of the AAT1 enzyme. **A**, Purified AAT1 proteins were treated with various concentrations of SNP (0, 50, 100, or 200 μM) for 2 h or with SNP (200 μM) for 1 h and then DTT (100 μM) for 1 h. The purified protein AAT activity was detected by colorimetric assay (n = 6). **B** and **C**, 100 μM SNP or ddH_2O treatment for 30 min at 37°C. The Eadie-Hofstee plot graphing was used to determine Vmax and Km values of purified AAT1 protein (n = 6). $^{**}P < 0.01$. Data are expressed as mean ± SEM. "V" means the reaction velocity. "[S](uM)" means the substrate concentration. AAT, aspartate aminotransferase; DTT, dithiothreitol; NO, nitric oxide; SNP, sodium nitroprusside.

with 50, 100, and 200 μM SNP were decreased by 37.76%, 74.03%, and 92.29%, compared to control treatment, respectively ($P < 0.01$) (Fig. 3A). The SO_2 fluorescence signal was attenuated in primary HASMCs after 100 μM SNP treatment compared to control treatment; the results are consistent with those of the HPLC quantitative analysis (Fig. 3B). The above results indicate that NO could inhibit endogenous SO_2 production in primary HASMCs.

To further examine the mechanisms by which NO inhibits endogenous SO_2 production in primary HASMCs, the expression level of AAT1, an endogenous SO_2 producing enzyme, was examined in primary HASMCs, and the results showed no significant difference in AAT1 protein expression in primary HASMCs after treatment with different concentrations of SNP (Fig. 3C). However, 50, 100, and 200 μM SNP treatment reduced AAT1 activity in primary HASMCs by 33.84% ($P < 0.05$), 48.42% ($P < 0.01$), and 63.21% ($P < 0.01$) compared to control treatment, respectively, while dithiothreitol (DTT; a thiol reducing agent) treatment blocked the effect of NO on AAT1 activity ($P < 0.01$) (Fig. 3D). The above results indicate that exogenous NO has no effect on the expression of AAT1 protein in primary HASMCs but represses AAT1 activity, suggesting that NO could inhibit endogenous SO_2 production by suppressing AAT1 activity in primary HASMCs.

3.4. *eNOS knockdown facilitates endogenous SO_2 production by promoting AAT1 activity in primary HASMCs*

A co-culture model of primary HAECs and primary HASMCs was used to determine the influence of HAEC-derived NO on endogenous SO_2 production in primary HASMCs. The results showed that in primary HAECs, eNOS protein expression was significantly reduced after knockdown of eNOS ($P < 0.01$) (Fig. 4A), and the NO level in the cell supernatant was reduced by 52.42% ($P < 0.01$) (Fig. 4B); however, the SO_2 level in the supernatant of primary HASMCs in co-culture primary HAECs and primary HASMCs was increased by 52.34% ($P < 0.01$) (Fig. 4C). The results of the SO_2 fluorescence probe in primary HASMCs are consistent with the HPLC results, which also showed increased endogenous SO_2 production after knockdown of eNOS expression (Fig. 4D). These results suggest that reduced NO production from primary HAECs could enhance endogenous SO_2 production in primary HASMCs. Further, knockdown of HAEC eNOS in the co-culture system did not impact AAT1 protein expression in primary HASMCs, but HASMC AAT1 activity was significantly increased after knockdown of HAEC eNOS ($P < 0.01$) (Fig. 4E and F). The findings indicate that reduced HAEC NO production could enhance AAT activity in primary HASMCs but did not affect AAT1 protein expression, suggesting that NO from primary HAECs could inhibit endogenous SO_2 production in primary HASMCs by suppressing AAT activity.

3.5. *NO directly inhibits purified protein AAT1 activity and affects kinetic characteristics of AAT1*

Different concentrations of SNP (50,100, and 200 μM) could significantly inhibit the activity of purified protein AAT1, and the inhibition rates were 20.53%, 45.32%, and 60.02%, respectively ($P < 0.01$); however, further application of DTT blocked the effect of SNP on AAT1 activity ($P < 0.01$) (Fig. 5A). The enzyme kinetic analysis showed that the Vmax value of purified AAT1 protein was decreased by 41.23% ($P < 0.01$), and the Km value was increased by 53.84% ($P < 0.05$) after treatment with 100 μM NO for 30 min (Fig. 5B and C). These results indicate that NO significantly inhibits the enzymatic catalytic efficiency of AAT1 (Vmax/Km).

3.6. *NO inhibits AAT1 activity through S-nitrosylation*

In vitro experiments revealed that DTT was able to reverse the effect of NO on AAT1 activity (Figs. 3D and 5A), suggesting that the cysteine sulfhydryl group of AAT1 protein might be the target of NO to inhibit endogenous AAT1 activity. The sulfhydryl S-nitrosylation modification, a covalent reaction of NO with the active cysteine on the target protein, is the main mechanism by which NO exerts its biological activity [31]. To further elucidate the molecular mechanism underlying inhibition of AAT1 protein activity by NO, we examined the S-nitrosylation level of AAT1 protein in primary HASMCs using a biotin switch assay. The results showed that the S-nitrosylation level of AAT1 protein was elevated in primary HASMCs after SNP treatment compared to control treatment, whereas application of DTT successfully blocked S-nitrosylation of AAT1 by NO ($P < 0.01$) (Fig. 6A). In addition, SNP treatment also increased the

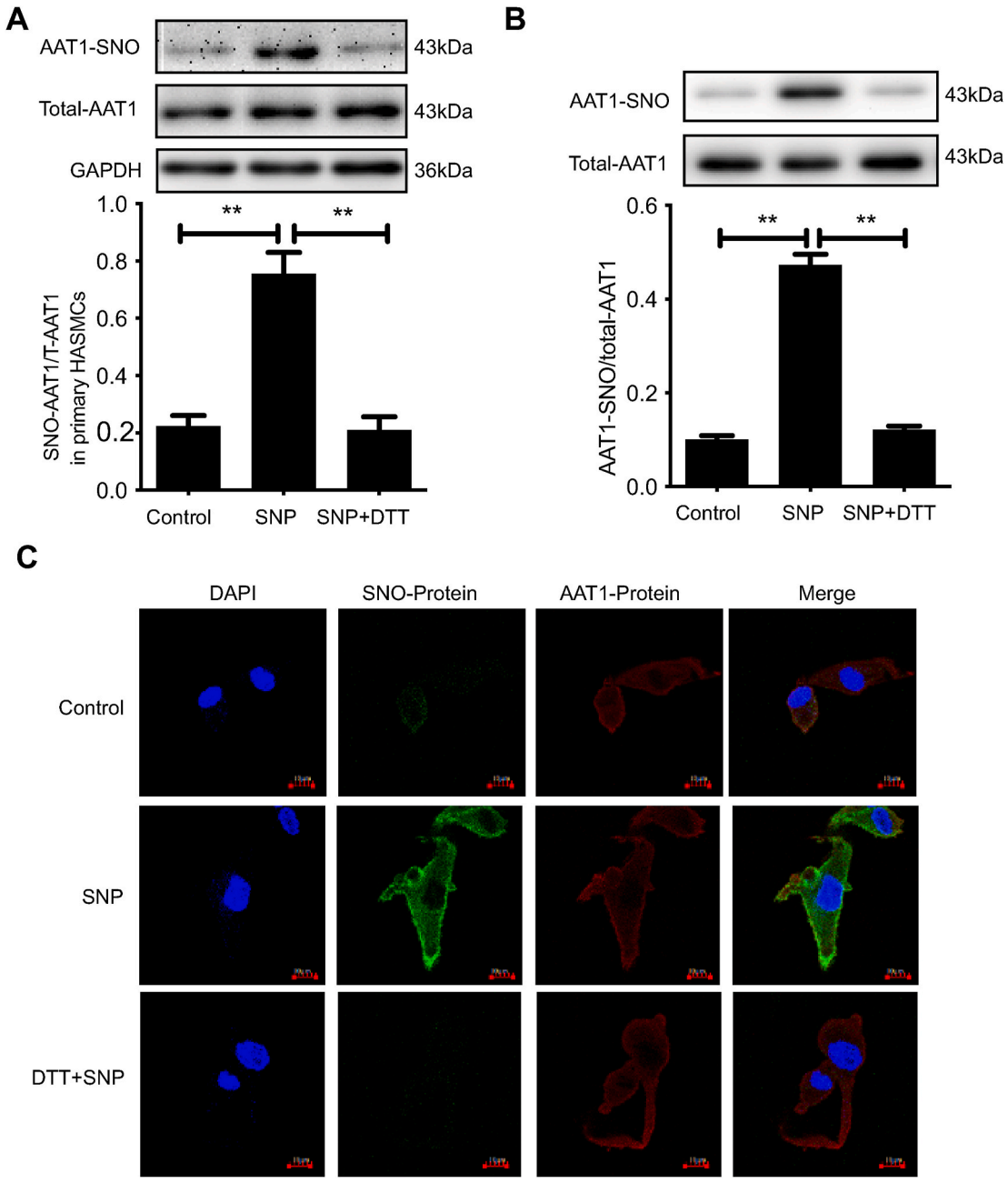

Fig. 6. NO inhibits AAT1 activity through S-nitrosylation. **A**, Primary HASMCs were treated with 100 μM of SNP for 2 h or with SNP (100 μM) for 1 h and then DTT (100 μM) for 1 h. The BSA method was used to detect nitrosylated AAT1 in primary HASMCs. **B**, Purified proteins were treated with 100 μM of SNP for 2 h or with SNP (100 μM) for 1 h and then DTT (100 μM) for 1 h. The BSA assay was used to detect S-nitrosylation of purified AAT1 protein. **C**, Primary HASMCs were treated with 100 μM of SNP for 2 h or with SNP (100 μM) for 1 h and then DTT (100 μM) for 1 h. *In situ* detection of AAT1 in primary HASMCs was performed by the fluorescent probe method. The nucleus is indicated by blue fluorescence, S-nitrosylation-modified protein by green fluorescence, AAT1 protein by red fluorescence, and S-nitrosylation-modified AAT1 protein by yellow fluorescence. Scale bar, 10 μm. n = 9–13.$^{**}P < 0.01$. Data are expressed as mean ± SEM. AAT, aspartate aminotransferase; DTT, dithiothreitol; NO, nitric oxide; SNP, sodium nitroprusside. (For interpretation of the references to color in this figure legend, the reader is referred to the Web version of this article.)

S-nitrosylation level of AAT1 in purified protein, and DTT treatment successfully blocked S-nitrosylation of AAT1 in purified protein by NO ($P < 0.01$) (Fig. 6B). In-situ inspection of AAT1 S-nitrosylation levels in primary HASMCs using a fluorescent probe method also yielded the consistent conclusion that SNP promotes AAT1 nitrosylation in primary HASMCs, whereas DTT markedly blocks AAT1 S-nitrosylation (Fig. 6C).

3.7. NO nitrosylates AAT1 at cysteine 192

Next, we examined the nitrosylation and the site of action of NO on purified AAT1 protein by LC-MS/MS, and the results showed that NO could nitrosylate AAT1 protein; the finding is consistent with the results of the BSA method and the fluorescence co-localization method mentioned above. S-nitrosylation on Cysteine 192 on the AAT1 protein was successfully detected, and Cysteine 192 of AAT1 was labeled by the Biotin-HPDP (428.19104 Da) probe with an *m/z* value of y_{15}^{2+}1042.19 (Fig. 7A), indicating that Cys192 is an S-nitrosylation site on AAT1 protein. To further determine the significance of NO-induced S-nitrosylation of Cys192 on AAT1, primary HASMCs were transfected with AAT1-C192S or AAT1-WT plasmid. The results showed that NO

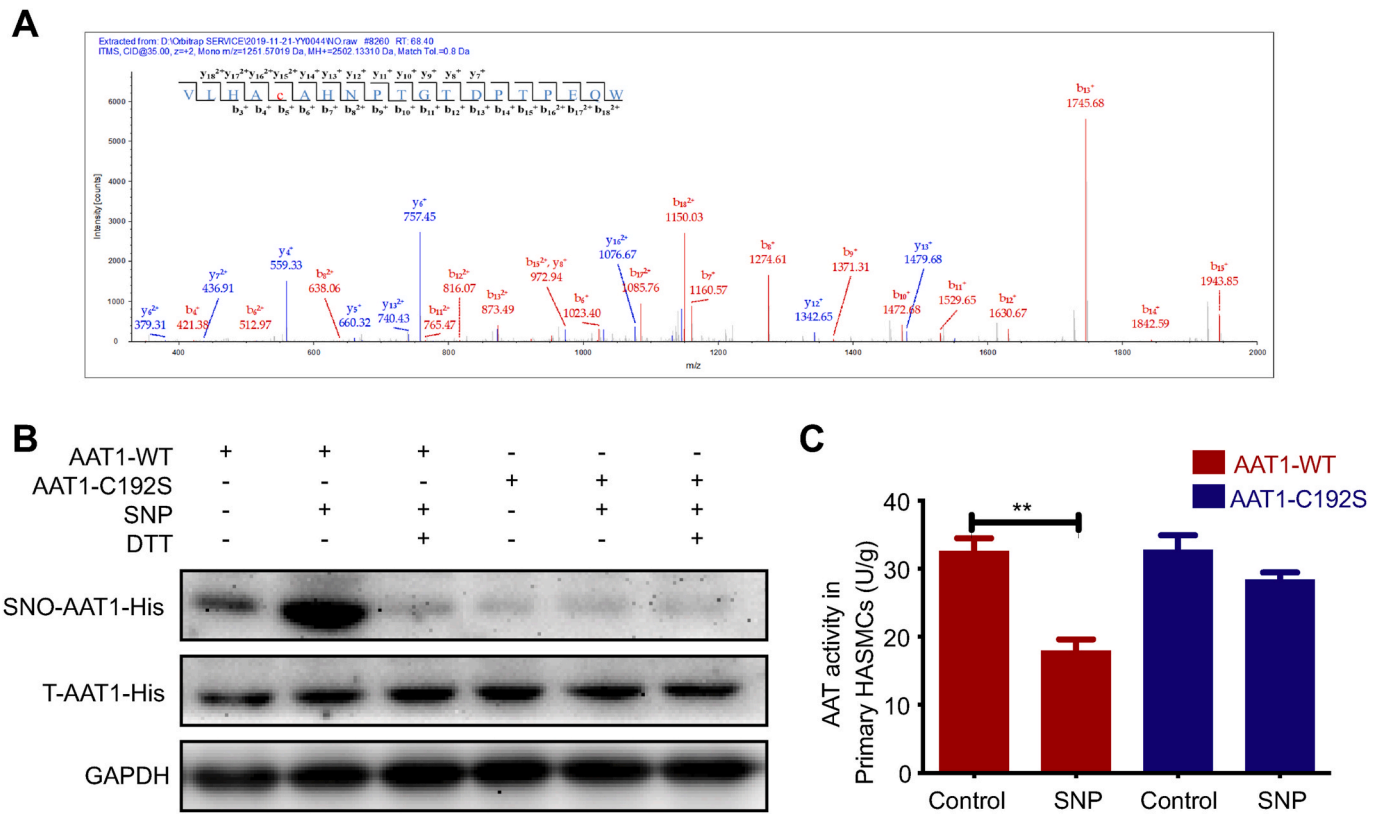

Fig. 7. NO nitrosylates AAT1 at Cys192. **A**, Effect of NO on the S-nitrosylation modified site of purified AAT1 protein. **B**, Primary HASMCs were treated with 100 μM SNP for 2 h or with SNP (100 μM) for 1 h and then DTT (100 μM) for 1 h after transfection with plasmid. The BSA method was used to detect S-nitrosylation modification of AAT1 protein Cys192 in primary HASMCs (n = 10). **C**, Primary HASMCs were treated with 100 μM of SNP for 2 h after transfection with plasmids, and AAT1-WT and AAT1-C192S activities in primary HASMCs were detected by colorimetric assay (n = 12). **P < 0.01. Data are expressed as mean ± SEM. AAT, aspartate aminotransferase; DTT, dithiothreitol; NO, nitric oxide; SNP, sodium nitroprusside.

nitrosylated AAT1 and inhibited the activity of AAT in primary HASMCs transfected with the AAT1-WT plasmid; in contrast, NO could not nitrosylate AAT1 and thereby not impact the activity of AAT in primary HASMCs transfected with the AAT1-C192S plasmid (Fig. 7B and C). These findings suggest that NO modifies the AAT1 Cys192 site by S-nitrosylation and thus inhibits the enzymatic activity of AAT1.

4. Discussion

This study reveals that the endogenous SO_2 pathway in HASMCs acts as a compensatory defense system against vascular remodeling and hypertension formation in response to the disturbed endogenous HAEC NO pathway, and NO inhibits AAT1 activity through S-nitrosylation modification of the Cys192 site of AAT1 protein, thereby reducing SO_2 production. This study is the first to demonstrate that HAEC-derived NO inhibits HASMC-derived SO_2 production, thereby contributing to a HAEC-HASMC communication mechanism.

NO is the first gas signaling molecule identified to be involved in signal transduction *in vivo*, and it is extremely easy to pass through the cell membrane and can diffuse freely inside and outside the cell. In the cardiovascular system, NO is produced by the endothelium and then diffuses rapidly outward, and it can induce smooth muscle cell relaxation in the vascular system, thereby causing vasodilation and calming blood pressure [32,33]. HAECs and HASMCs are the main cellular components of the vascular wall, and the information interaction between the two types of cells plays a significant role in vascular physiological homeostasis and pathological vascular reshaping. Since gaseous signaling molecules can easily diffuse and penetrate the intercellular space and multiple gaseous signaling molecules are involved in the adjustment of intravascular homeostasis and blood pressures, we hypothesized that gaseous signaling molecules NO and SO_2 communicate between HAECs and HASMCs. Therefore, we investigated the relationship between NO and SO_2 using an animal model of L-NAME--induced hypertension as well as a co-culture model of HAECs-HASMCs. In L-NAME-induced hypertensive mice, the AAT activity of the mouse aortic tissue was decreased, and plasma SO_2 content was reduced. Administration of HDX resulted in further increased vascular remodeling in the aorta and arterioles, and blood pressure. *In vitro*, SNP could inhibit the AAT activity of HASMCs and decrease the SO_2 level in the supernatant in HASMCs, while knockdown of eNOS in HAECs could increase the SO_2 level in the supernatant of HASMCs, suggesting that NO derived from HAECs could inhibit SO_2 production in HASMCs. We speculate that the effect of HAEC-derived NO on HASMC-derived SO_2 production might be a molecular mechanism underlying the communication between HAECs and HASMCs.

The mechanisms underlying the inhibitory effect of HAECs-derived NO on HASMC-derived SO_2 production remain unclear. Endogenous production of SO_2 is mainly regulated by protein expression and activity of its key regulation enzyme AAT1. We investigated the modulatory effect of HAEC-derived NO on the HASMC-derived SO_2/AAT1 pathway under various physiological conditions in a co-culture model of HAECs and HASMCs. The results showed that HAECs-derived NO had no impact on AAT1 gene expression in HASMCs but regulated protease activity, a relatively faster and better controllable factor. As expected, we confirmed the direct regulatory effect of NO on the enzymatic reaction of AAT1 in our experiments with purified AAT1 protein. NO decreased the Vmax value and increased the Km value of AAT1, suggesting that NO may reduce the enzyme-substrate affinity and the number of bound substrates by altering the structure of AAT1 protein, which in turn severely reduces the catalytic efficiency (Vmax/Km) of AAT1 enzyme.

The finding demonstrates that NO can directly inhibit the activity of AAT1. Further, the S-nitrosylation level of AAT1 was examined in purified AAT1 protein and HASMCs using the BSA method. We found that NO could nitrosylate AAT1 protein, and DTT treatment could significantly eliminate S-nitrosylation modification of AAT1 protein by NO, indicating that NO acts on the sulfhydryl group of AAT1 by S-nitrosylation modification and inhibits AAT activity. Notably, a previous study showed that SO_2 could inhibit AAT activity by modifying the AAT1 Cys192 site through sulfenylation [34]. Moreover, homologous sequence analysis revealed that Cys192 of AAT1 protein is highly conserved, and NO might nitrosylate AAT1 on the Cys192 site. To further confirm this hypothesis, using LC-MS/MS, we examined whether NO can nitrosylate AAT1 protein and what the possible sites of action are. We found that NO did nitrosylate AAT1 protein, as demonstrated by the BSA method and fluorescence co-localization method mentioned above, and Cys192 was the S-nitrosylation modification site, suggesting that Cys192 is a molecular target of NO for chemical modification of AAT1 protein and regulation of its activity. Thus, NO might inhibit AAT1 activity by S-nitrosylation modification of AAT1 Cys192.

Endogenous SO_2 in the cardiovascular system, as an emerging gas transmitter, has important effects on blood pressure regulation and inhibition of vascular structural remodeling [35–38]. In the present study, we detected blood pressure by the tail-cuff method and implantable telemetry in the L-NAME-induced hypertension model mice and found that endogenous SO_2 levels were elevated, and blood pressure was elevated in these mice when the NO/NOS pathway was impaired. HDX administration further aggravated vascular remodeling and blood pressure, suggesting that endogenous SO_2 acts as a compensatory defense system of the disturbed endogenous NO pathway and antagonizes hypertension in response to injury stimuli. Moreover, in the HAEC-HASMC co-culture cell model, it was found that when the HAEC-derived NO/NOS pathway was impaired, SO_2 production and collagen III protein expression in HASMCs were elevated. However, the addition of HDX, a key enzyme inhibitor of SO_2 production, further increased collagen III protein expression in HASMCs, suggesting that decreased HAECs-derived NO can maintain normal vascular structure by increasing the production of HASMC-derived SO_2. The findings indicate that the HASMC-derived SO_2 pathway acts as a compensatory defense system of the disturbed HAEC-derived NO pathway to antagonize the development of hypertension and vascular structural remodeling.

In conclusion, this study is the first to demonstrate that the endogenous SO_2 pathway is involved in the regulation of cardiovascular homeostatic balance as a defense mechanism against the disturbed endogenous NO system under pathological conditions. The inhibition of HASMC-derived SO_2 production by HAEC-derived NO is a novel molecular mechanism for HAEC-HASMC intercellular communication.

Sources of funding

This study was supported by National Natural Science Foundation of China (81770278, 81770422, 82070445, 81921001, 81970424), Beijing Municipal Natural Science Foundation (7191012).

Disclosures

None.

Declaration of competing interest

The authors declare that they have no conflict of interest.

Acknowledgments

Hongfang Jin, Junbao Du, Chaoshu Tang and Yaqian Huang designed the research. Yunjia Song, Jiaru Song, Zhigang Zhu, Hanlin Peng, Xiang Ding, Guosheng Yang, Kun Li, Xiaoqi Yu, Yinghong Tao and Dingfang Bu performed the experiments. Yunjia Song, Jiaru Song, Guosheng Yang, Hongfang Jin, Junbao Du and Yaqian Huang analyzed the data. Kun Li, Xiaoqi Yu and Dingfang Bu provided technical support. Jiaru Song, Junbao Du and Hongfang Jin wrote the manuscript. Hongfang Jin, Junbao Du, Chaoshu Tang and Yaqian Huang revised the manuscript. All authors read and approved the final manuscript.

References

[1] P.M. Kearney, M. Whelton, K. Reynolds, P. Muntner, P.K. Whelton, J. He, Global burden of hypertension: analysis of worldwide data, Lancet. 365 (2005) 217–223.
[2] S. Oparil, M.C. Acelajado, G.L. Bakris, D.R. Berlowitz, R. Cifkova, A.F. Dominiczak, G. Grassi, J. Jordan, N.R. Poulter, A. Rodgers, P.K. Whelton, Hypertension, Nat. Rev. Dis. Primers. 4 (2018) 18014.
[3] R.M. Rapoport, M.B. Draznin, F. Murad, Endothelium-dependent relaxation in rat aorta may be mediated through cyclic GMP-dependent protein phosphorylation, Nature. 306 (1983) 174–176.
[4] U. Forstermann, A. Mulsch, E. Bohme, R. Busse, Stimulation of soluble guanylate cyclase by an acetylcholine-induced endothelium-derived factor from rabbit and canine arteries, Circ. Res. 58 (1986) 531–538.
[5] L.J. Ignarro, R.G. Harbison, K.S. Wood, P.J. Kadowitz, Activation of purified soluble guanylate cyclase by endothelium-derived relaxing factor from intrapulmonary artery and vein: stimulation by acetylcholine, bradykinin and arachidonic acid, J. Pharmacol. Exp. Therapeut. 237 (1986) 893–900.
[6] P.L. Huang, Z. Huang, H. Mashimo, K.D. Bloch, M.A. Moskowitz, J.A. Bevan, M. C. Fishman, Hypertension in mice lacking the gene for endothelial nitric oxide synthase, Nature. 377 (1995) 239–242.
[7] D.D. Rees, R.M. Palmer, S. Moncada, Role of endothelium-derived nitric oxide in the regulation of blood pressure, Proc. Natl. Acad. Sci. U. S. A. 86 (1989) 3375–3378.
[8] P. Forte, M. Copland, L.M. Smith, E. Milne, J. Sutherland, N. Benjamin, Basal nitric oxide synthesis in essential hypertension, Lancet. 349 (1997) 837–842.
[9] H. Jin, Y. Wang, X. Wang, Y. Sun, C. Tang, J. Du, Sulfur dioxide preconditioning increases antioxidative capacity in rat with myocardial ischemia reperfusion (I/R) injury, Nitric. Oxide. 32 (2013) 56–61.
[10] X.B. Wang, J.B. Du, H. Cui, Signal pathways involved in the biological effects of sulfur dioxide, Eur. J. Pharmacol. 764 (2015) 94–99.
[11] Y. Sun, Y. Tian, M. Prabha, D. Liu, S. Chen, R. Zhang, X. Liu, C. Tang, X. Tang, H. Jin, J. Du, Effects of sulfur dioxide on hypoxic pulmonary vascular structural remodeling, Lab. Invest. 90 (2010) 68–82.
[12] W. Li, C. Tang, H. Jin, J. Du, Regulatory effects of sulfur dioxide on the development of atherosclerotic lesions and vascular hydrogen sulfide in atherosclerotic rats, Atherosclerosis. 215 (2011) 323–330.
[13] X.B. Wang, X.M. Huang, T. Ochs, X.Y. Li, H.F. Jin, C.S. Tang, J.B. Du, Effect of sulfur dioxide preconditioning on rat myocardial ischemia/reperfusion injury by inducing endoplasmic reticulum stress, Basic Res. Cardiol. 106 (2011) 865–878.
[14] Y. Huang, H. Zhang, B. Lv, C. Tang, J. Du, H. Jin, Endogenous sulfur dioxide is a new gasotransmitter with promising therapeutic potential in cardiovascular system, Sci. Bull. 66 (2021) 1604–1607.
[15] Y. Huang, C. Tang, J. Du, H. Jin, Endogenous sulfur dioxide: a new member of gasotransmitter family in the cardiovascular system, Oxid. Med. Cell. Longev. 2016 (2016) 8961951.
[16] D. Liu, H. Jin, C. Tang, J. Du, Sulfur dioxide: a novel gaseous signal in the regulation of cardiovascular functions, Mini Rev. Med. Chem. 10 (2010) 1039–1045.
[17] S.X. Du, H.F. Jin, D.F. Bu, X. Zhao, B. Geng, C.S. Tang, J.B. Du, Endogenously generated sulfur dioxide and its vasorelaxant effect in rats, Acta Pharmacol. Sin. 29 (2008) 923–930.
[18] D. Liu, Y. Huang, D. Bu, A.D. Liu, L. Holmberg, Y. Jia, C. Tang, J. Du, H. Jin, Sulfur dioxide inhibits vascular smooth muscle cell proliferation via suppressing the ERK/MAP kinase pathway mediated by cAMP/PKA signaling, Cell. Death. Dis. 5 (2014) e1251.
[19] X. Zhao, H.F. Jin, C.S. Tang, J.B. Du, Effect of sulfur dioxide on vascular collagen remodeling in spontaneously hypertensive rats, Zhonghua. Er. Ke. Za. Zhi. 46 (2008) 905–908.
[20] Q. Yao, Y. Huang, A.D. Liu, M. Zhu, J. Liu, H. Yan, Q. Zhang, B. Geng, Y. Gao, S. Du, P. Huang, C. Tang, J. Du, H. Jin, The vasodilatory effect of sulfur dioxide via sGC/cGMP/PKG pathway in association with sulfhydryl-dependent dimerization, Am. J. Physiol. Regul. Integr. Comp. Physiol. 310 (2016) R1073–R1080.
[21] J.H. Yang, C.S. Pan, Y.X. Jia, J. Zhang, J. Zhao, Y.Z. Pang, J. Yang, C.S. Tang, Y. F. Qi, Intermedin1-53 activates L-arginine/nitric oxide synthase/nitric oxide pathway in rat aortas, Biochem. Biophys. Res. Commun. 341 (2006) 567–572.
[22] K. Kimura, K. Tsuda, A. Baba, T. Kawabe, S. Boh-oka, M. Ibata, C. Moriwaki, T. Hano, I. Nishio, Involvement of nitric oxide in endothelium-dependent arterial relaxation by leptin, Biochem. Biophys. Res. Commun. 273 (2000) 745–749.
[23] A. Mas-Capdevila, L. Iglesias-Carres, A. Arola-Arnal, G. Aragones, A. Aleixandre, F. I. Bravo, B. Muguerza, Evidence that nitric oxide is involved in the blood pressure lowering effect of the peptide avfqhncqe in spontaneously hypertensive rats, Nutrients. 11 (2019) 255.
[24] C. Farah, L.Y.M. Michel, J.L. Balligand, Nitric oxide signalling in cardiovascular health and disease, Nat. Rev. Cardiol. 15 (2018) 292–316.
[25] J. Li, Z. Meng, The role of sulfur dioxide as an endogenous gaseous vasoactive factor in synergy with nitric oxide, Nitric. Oxide. 20 (2009) 166–174.

[26] W. Lu, Y. Sun, C. Tang, T. Ochs, J. Qi, J. Du, H. Jin, Sulfur dioxide derivatives improve the vasorelaxation in the spontaneously hypertensive rat by enhancing the vasorelaxant response to nitric oxide, Exp. Biol. Med. 237 (2012) 867–872.
[27] D. Zhang, X. Wang, X. Tian, L. Zhang, G. Yang, Y. Tao, C. Liang, K. Li, X. Yu, X. Tang, C. Tang, J. Zhou, W. Kong, J. Du, Y. Huang, H. Jin, The increased endogenous sulfur dioxide acts as a compensatory mechanism for the downregulated endogenous hydrogen sulfide pathway in the endothelial cell inflammation, Front. Immunol. 9 (2018) 882.
[28] J. Yang, K. Li, J.T. Hou, C.Y. Lu, L.L. Li, K.K. Yu, X.Q. Yu, A novel coumarin-based water-soluble fluorescent probe for endogenously generated SO_2 in living cells, Sci. China. Chem. 60 (2017) 793–798.
[29] S. Keiding, S. Johansen, N. Tygstrup, Galactose removal kinetics during hypoxia in perfused pig liver: reduction of Vmax, but not of intrinsic clearance Vmax/Km, Eur. J. Clin. Invest. 20 (1990) 305–309.
[30] G. Zhong, F. Chen, Y. Cheng, C. Tang, J. Du, The role of hydrogen sulfide generation in the pathogenesis of hypertension in rats induced by inhibition of nitric oxide synthase, J. Hypertens. 21 (2003) 1879–1885.
[31] D.T. Hess, A. Matsumoto, S.O. Kim, H.E. Marshall, J.S. Stamler, Protein S-nitrosylation: purview and parameters, Nat. Rev. Mol. Cell Biol. 6 (2005) 150–166.
[32] L.J. Ignarro, G.M. Buga, K.S. Wood, R.E. Byrns, G. Chaudhuri, Endothelium-derived relaxing factor produced and released from artery and vein is nitric oxide, Proc. Natl. Acad. Sci. U. S. A. 84 (1987) 9265–9269.
[33] H. Li, K. Witte, M. August, I. Brausch, U. Godtel-Armbrust, A. Habermeier, E. I. Closs, M. Oelze, T. Munzel, U. Forstermann, Reversal of endothelial nitric oxide synthase uncoupling and up-regulation of endothelial nitric oxide synthase expression lowers blood pressure in hypertensive rats, J. Am. Coll. Cardiol. 47 (2006) 2536–2544.
[34] Y. Song, H. Peng, D. Bu, X. Ding, F. Yang, Z. Zhu, X. Tian, L. Zhang, X. Wang, C. Tang, Y. Huang, J. Du, H. Jin, Negative auto-regulation of sulfur dioxide generation in vascular endothelial cells: AAT1 S-sulfenylation, Biochem. Biophys. Res. Commun. 525 (2020) 231–237.
[35] W. Yu, D. Liu, C. Liang, T. Ochs, S. Chen, S. Chen, S. Du, C. Tang, Y. Huang, J. Du, H. Jin, Sulfur dioxide protects against collagen accumulation in pulmonary artery in association with downregulation of the transforming growth factor beta1/smad pathway in pulmonary hypertensive rats, J. Am. Heart. Assoc. 5 (2016) e003910.
[36] Y. Huang, Z. Li, L. Zhang, H. Tang, H. Zhang, C. Wang, S.Y. Chen, D. Bu, Z. Zhang, Z. Zhu, P. Yuan, K. Li, X. Yu, W. Kong, C. Tang, Y. Jung, R.B. Ferreira, K.S. Carroll, J. Du, J. Yang, H. Jin, Endogenous SO_2-dependent smad3 redox modification controls vascular remodeling, Redox. Biol. 41 (2021) 101898.
[37] Y. Huang, Z. Shen, Q. Chen, P. Huang, H. Zhang, S. Du, B. Geng, C. Zhang, K. Li, C. Tang, J. Du, H. Jin, Endogenous sulfur dioxide alleviates collagen remodeling via inhibiting TGF-beta/Smad pathway in vascular smooth muscle cells, Sci. Rep. 6 (2016) 19503.
[38] L. Luo, X. Hong, B. Diao, S. Chen, M. Hei, Sulfur dioxide attenuates hypoxia-induced pulmonary arteriolar remodeling via DKK1/WNT signaling pathway, Biomed. Pharmacother. 106 (2018) 692–698.